Advanced Robotics, Vol. 18, No. 1, pp. 23–44 (2004)

Also available online - www.vsppub.com

Full paper

Task-based compliance planning for multi-fingered robotic manipulations

BYOUNG-HO KIM [1], BYUNG-JU YI [2,*], SANG-ROK OH [3] and IL HONG SUH [2]

[1] *Department of Robotics, Ritsumeikan University, Kusatsu, Shiga, Japan*
[2] *School of Electrical Engineering and Computer Science, Hanyang University, 1271 Sa 1-dong, Ansan, Sangrok-gu, Kyunghi-do 426-791, South Korea*
[3] *Intelligent System Control Research Center, KIST, Seoul, South Korea*

Received 25 February 2003; accepted 28 May 2003

Abstract—Based on the analysis of the stiffness relation between the operational space and the fingertip space of multi-fingered hands, this paper provides a guideline of task-based compliance planning for multi-fingered robotic manipulations. In order to show the characteristics of the task-based stiffness matrix, various two- and three-dimensional examples are illustrated. Also, it is shown that some of the coupling stiffness elements cannot be planned arbitrarily due to grasping geometry. Through the analytical results, it is concluded that the operational stiffness matrix should be carefully specified by considering the location of the compliance center and the grasp geometry of multi-fingered hands for successful grasping and manipulation tasks.

Keywords: Multi-fingered robotic manipulation; compliance planning; grasp geometry.

1. INTRODUCTION

Several explicit force-based techniques have been proposed for effective grasping and manipulation of an object by multi-fingered hands, or multiple robot arms [1–3]. Implementation of those methods may suffer from attaching force sensors in small finger mechanisms, as well as processing noisy force signals. Also, the integration of tactile and force information for individual finger control, and the combination of information from different fingers to guide the hand action, are still not well known [4]. Thus, instead of employing force signals, compliance has been known as a successful alternative for characterizing the grasping and manipulation of robot hands [5–7]. In particular, when an object grasped by a multi-fingered

*To whom correspondence should be addressed. E-mail: bj@hanyang.ac.kr

hand is being manipulated in a constrained space, appropriate compliance planning of the hand may be crucial for successful compliant tasks [8–10].

Related to grasp stiffness or compliance, Cutkosky *et al.* [5] analyzed the effective grasp stiffness by considering the structural compliances in fingers and fingertips, servo gains at the joints of the finger, and small changes in the grasp geometry that may affect the grasp forces acting upon the object. Also, Kaneko *et al.* [6] and Kao *et al.* [7] tried to apply stiffness models usually employed in robotics research to the analysis of stable grasping behaviors. Kim *et al.* [11] proposed an independent finger/joint-based compliance control method for robot hands manipulating an object and also addressed the geometric condition for successful implementation of a compliance control scheme. Some researchers have investigated the task-based stiffness characteristics with respect to the task motion constraints [12–14]. They pointed out that the diagonal stiffness elements can be determined by considering the task characteristics for each direction. In Ref. [15], a methodology specifying and achieving passive compliance for a remote center of compliance (RCC) device was proposed. However, that approach is based on passive compliance attached to a manipulator, but not related to multi-fingered hands. It is also pointed out that a stiffness matrix containing some off-diagonal terms can be useful to prevent the jamming of contact tasks. In Ref. [16], the fundamentals of compliance characteristics for multi-fingered hands were been analyzed. It was shown that some of the coupling stiffness elements cannot be planned arbitrarily and a five-fingered hand is necessary to implement a 6×6 operational stiffness matrix by using an independent finger-based compliance control method which is effective to achieve the specified compliance characteristics. They also pointed out that the operational stiffness matrix should be carefully specified in consideration of the grasp geometry of multi-fingered hands for successful grasping and manipulation tasks. Recently, many research groups have investigated the synthesis of planar and spatial stiffness matrices based on the placement of passive springs [17–19]. However, these previous studies were confined to passive spring mechanisms and were not directly related to multi-fingered hands. Also, task-based analysis for specifying compliance characteristics by considering the grasp geometry and the compliance center is still an open research field.

The objective of this paper is to provide task-based guidelines for specifying compliance characteristics of multi-fingered hands through an investigation of the stiffness relation between the operational space and the fingertip space based on the grasp geometry. The theoretical background will be based on the independent compliance control algorithm proposed in Ref. [11] in which a simple hybrid control was treated as an illustrative example and thus the applicability of the scheme was not fully demonstrated. In this study, we will demonstrate general application examples through which a guideline for task-based stiffness control will be suggested.

The procedure of this study is as follows. In order to provide the theoretical background of this work, Section 2 describes the stiffness relation between the

operational space and the fingertip space. Then, we present compliance planning for planar and three-dimensional (3D) assembly tasks in Section 3. Next, compliance planning for hand-writing tasks is shown in Section 4. Finally, concluding remarks are given in Section 5.

2. INDEPENDENT STIFFNESS RELATION OF MULTI-FINGERED MANIPULATIONS

The stiffness or compliance can be employed to characterize the grasping and manipulation of robot hands in the case that it is specially dominated in approximated linear analysis where low velocities and small relative motions lead to small inertial forces. In this section, we present the stiffness relation between the operational space and the fingertip space of multi-fingered manipulating systems.

Consider a rigid object being manipulated by a n_{f}-fingered robot hand as shown in Fig. 1, where each finger has ${}^{i}n_{\mathrm{j}}$-joints, and the relation between the generalized force vector in the operational space and the fingertip force vector is given by:

$$T_{\mathrm{o}} = \left[\boldsymbol{G}_{\mathrm{o}}^{\mathrm{f}}\right]^{\mathrm{T}} T_{\mathrm{f}}, \tag{1}$$

where $T_{\mathrm{o}} \in \mathcal{R}^{n\times 1}$ denotes the generalized force vector in the operational space (o) including the inertial load and external load, the fingertip force vector $T_{\mathrm{f}} \in \mathcal{R}^{m\times 1}$ in the fingertip space (f) is expressed as:

$$T_{\mathrm{f}} = \left[\ \left({}^{1}T_{\mathrm{f}}\right)^{\mathrm{T}} \quad \left({}^{2}T_{\mathrm{f}}\right)^{\mathrm{T}} \quad \cdots \quad \left({}^{n_{\mathrm{f}}}T_{\mathrm{f}}\right)^{\mathrm{T}}\ \right]^{\mathrm{T}},$$

and the Jacobian matrix between the operational space and the fingertip space $[\boldsymbol{G}_{\mathrm{o}}^{\mathrm{f}}] \in \mathcal{R}^{m\times n}$ is given by:

$$\left[\boldsymbol{G}_{\mathrm{o}}^{\mathrm{f}}\right] = \left[\ \left[{}^{1}\boldsymbol{G}_{\mathrm{o}}^{\mathrm{f}}\right]^{\mathrm{T}} \quad \left[{}^{2}\boldsymbol{G}_{\mathrm{o}}^{\mathrm{f}}\right]^{\mathrm{T}} \quad \cdots \quad \left[{}^{n_{\mathrm{f}}}\boldsymbol{G}_{\mathrm{o}}^{\mathrm{f}}\right]^{\mathrm{T}}\ \right]^{\mathrm{T}},$$

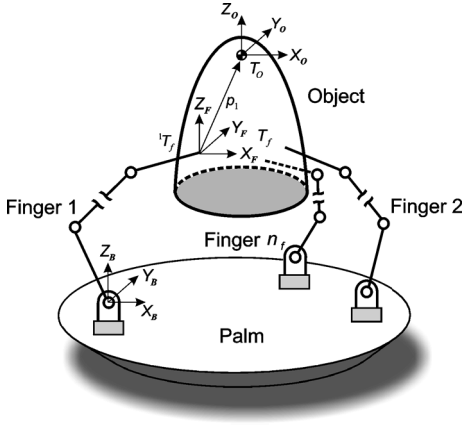

Figure 1. A multi-fingered manipulating system.

and:

$$\left[{}^{i}\boldsymbol{G}_{\mathrm{o}}^{\mathrm{f}}\right] = \begin{bmatrix} {}_{\mathrm{o}}^{\mathrm{f}}\boldsymbol{R}_i & {}_{\mathrm{o}}^{\mathrm{f}}p_i \times {}_{\mathrm{o}}^{\mathrm{f}}\boldsymbol{R}_i \\ 0 & {}_{\mathrm{o}}^{\mathrm{f}}\boldsymbol{R}_i \end{bmatrix}.$$

Here, ${}_{\mathrm{o}}^{\mathrm{f}}\boldsymbol{R}_i$ and ${}_{\mathrm{o}}^{\mathrm{f}}p_i$ denote the rotation matrix and the position vector from the operational space to the fingertip space, respectively. Also, m ($m = \sum_{i=1}^{n_{\mathrm{f}}} {}^{i}n_{\mathrm{fp}}$, where ${}^{i}n_{\mathrm{fp}}$ denotes the dimension of the ith fingertip) denotes the total dimension of wrenches applied to the grasped object by n_{f} fingers.

When the trajectory of the grasped object is pre-specified, the task of load distribution will be the determination of the fingertip forces and moments in order to achieve a desired motion of the object and to maintain the grasp. The general solution of (1) is given by:

$$T_{\mathrm{f}} = \left(\left[\boldsymbol{G}_{\mathrm{o}}^{\mathrm{f}}\right]^{\mathrm{T}}\right)^{+} T_{\mathrm{o}} + \left(\boldsymbol{I} - \left(\left[\boldsymbol{G}_{\mathrm{o}}^{\mathrm{f}}\right]^{\mathrm{T}}\right)^{+}\left[\boldsymbol{G}_{\mathrm{o}}^{\mathrm{f}}\right]^{\mathrm{T}}\right)\xi_f, \tag{2}$$

where the superscript T implies the transpose of a matrix, $([\boldsymbol{G}_{\mathrm{o}}^{\mathrm{f}}]^{\mathrm{T}})^{+}$ is a pseudo-inverse of $[\boldsymbol{G}_{\mathrm{o}}^{\mathrm{f}}]^{\mathrm{T}}$ and ξ_{f} is an arbitrary $m \times 1$ vector. $\boldsymbol{I}$ denotes an $m \times m$ identity matrix.

Using (2), we can perform explicit force control of robot hands by using force sensor signals, but the motion control of the fingers is difficult in practice because hardware implementation of the force sensor is very costly and not easy, and the real force signal is very noisy. Therefore, the stiffness or compliance control method would be very effective in robot hand operations, compared to the explicit force control method.

By using the duality principle, the velocity relation between the operational space and the fingertip space can be given by:

$$\frac{\partial u_{\mathrm{f}}}{\partial u_{\mathrm{o}}} = \left[\boldsymbol{G}_{\mathrm{o}}^{\mathrm{f}}\right], \tag{3}$$

where u_{f} and u_{o} denote the $3n_{\mathrm{f}} \times 1$ displacement vector in the fingertip space and the 6×1 displacement vector in the operational space, respectively. Those vectors are given by:

$$u_{\mathrm{f}} = \left[\begin{array}{cccc} \left({}^{1}u_{\mathrm{f}}\right)^{\mathrm{T}} & \left({}^{2}u_{\mathrm{f}}\right)^{\mathrm{T}} & \cdots & \left({}^{n_{\mathrm{f}}}u_{\mathrm{f}}\right)^{\mathrm{T}} \end{array}\right]^{\mathrm{T}},$$

in which ${}^{i}u_{\mathrm{f}}$ ($i = 1, \ldots, n_{\mathrm{f}}$) is given by:

$${}^{i}u_{\mathrm{f}} = \left[{}^{i}u_{\mathrm{f}x}\ {}^{i}u_{\mathrm{f}y}\ {}^{i}u_{\mathrm{f}z}\right]^{\mathrm{T}},$$

and:

$$u_{\mathrm{o}} = [u_{\mathrm{o}x}\ u_{\mathrm{o}y}\ u_{\mathrm{o}z}\ u_{\mathrm{o}\gamma}\ u_{\mathrm{o}\beta}\ u_{\mathrm{o}\alpha}]^{\mathrm{T}},$$

where subscripts γ, β and α imply the rotational angles about the x-, y- and z-axis, respectively.

Then, by taking the partial derivative of (1) with respect to the 6×1 displacement vector u_{o} in the operational space and by using the chain rule, the $n \times n$ stiffness

matrix in the operational space, $[\boldsymbol{K}'_{\mathrm{o}}]$, can be expressed as follows:

$$\begin{aligned}\left[\boldsymbol{K}'_{\mathrm{o}}\right] &= -\frac{\partial T_{\mathrm{o}}}{\partial u_{\mathrm{o}}} \\ &= -\left[\boldsymbol{G}_{\mathrm{o}}^{\mathrm{f}}\right]^{\mathrm{T}} \frac{\partial T_{\mathrm{f}}}{\partial u_{\mathrm{f}}} \frac{\partial u_{\mathrm{f}}}{\partial u_{\mathrm{o}}} - \frac{\partial [\boldsymbol{G}_{\mathrm{o}}^{\mathrm{f}}]^{\mathrm{T}}}{\partial u_{\mathrm{o}}} T_{\mathrm{f}} \\ &= \left[\boldsymbol{G}_{\mathrm{o}}^{\mathrm{f}}\right]^{\mathrm{T}} [\boldsymbol{K}_{\mathrm{f}}] \left[\boldsymbol{G}_{\mathrm{o}}^{\mathrm{f}}\right] - \frac{\partial [\boldsymbol{G}_{\mathrm{o}}^{\mathrm{f}}]^{\mathrm{T}}}{\partial u_{\mathrm{o}}} T_{\mathrm{f}} \\ &= \left[\boldsymbol{G}_{\mathrm{o}}^{\mathrm{f}}\right]^{\mathrm{T}} [\boldsymbol{K}_{\mathrm{f}}] \left[\boldsymbol{G}_{\mathrm{o}}^{\mathrm{f}}\right] - \left([T_{\mathrm{f}}]^{\mathrm{T}} \circ \left[\boldsymbol{H}_{\mathrm{oo}}^{\mathrm{f}}\right]\right), \end{aligned} \tag{4}$$

where $[\boldsymbol{K}_{\mathrm{f}}]$, representing the $m \times m$ stiffness matrix in the fingertip space, is expressed as:

$$[\boldsymbol{K}_{\mathrm{f}}] = \begin{bmatrix} {}^{1}\boldsymbol{K}_{\mathrm{f}} & {}^{12}\boldsymbol{K}_{\mathrm{f}} & \cdots & {}^{1n_{\mathrm{f}}}\boldsymbol{K}_{\mathrm{f}} \\ {}^{21}\boldsymbol{K}_{\mathrm{f}} & {}^{2}\boldsymbol{K}_{\mathrm{f}} & \cdots & {}^{2n_{\mathrm{f}}}\boldsymbol{K}_{\mathrm{f}} \\ \vdots & \vdots & \ddots & \vdots \\ {}^{n_{\mathrm{f}}1}\boldsymbol{K}_{\mathrm{f}} & {}^{n_{\mathrm{f}}2}\boldsymbol{K}_{\mathrm{f}} & \cdots & {}^{n_{\mathrm{f}}}\boldsymbol{K}_{\mathrm{f}} \end{bmatrix},$$

in which $[{}^{i}\boldsymbol{K}_{\mathrm{f}}]$ $(i = 1, \ldots, n_{\mathrm{f}})$ is given by:

$$[{}^{i}\boldsymbol{K}_{\mathrm{f}}] = \begin{bmatrix} {}^{i}\boldsymbol{K}_{\mathrm{f}xx} & {}^{i}\boldsymbol{K}_{\mathrm{f}xy} & {}^{i}\boldsymbol{K}_{\mathrm{f}xz} \\ {}^{i}\boldsymbol{K}_{\mathrm{f}yx} & {}^{i}\boldsymbol{K}_{\mathrm{f}yy} & {}^{i}\boldsymbol{K}_{\mathrm{f}yz} \\ {}^{i}\boldsymbol{K}_{\mathrm{f}zx} & {}^{i}\boldsymbol{K}_{\mathrm{f}zy} & {}^{i}\boldsymbol{K}_{\mathrm{f}zz} \end{bmatrix},$$

specifically for the case of a point contact with friction, and ${}^{ij}\boldsymbol{K}_{\mathrm{f}}$ in $[\boldsymbol{K}_{\mathrm{f}}]$ denotes the inter-finger coupling stiffness matrix between the ith finger and the jth finger. The operator of $(\circ)$ and $[\boldsymbol{H}_{\mathrm{oo}}^{\mathrm{f}}]$, respectively, represent the Generalized Scalar Dot Product [20] and the second-order kinematic influence coefficient matrix, the latter representing the change of $[\boldsymbol{G}_{\mathrm{o}}^{\mathrm{f}}]$ with respect to contact configuration [21].

Note that the second term of (4) is not utilized in Salisbury's algorithm [22]. This becomes crucial when the magnitudes of the grasping forces T_{f} are considerable [21, 23, 24]. Since the second term of (4) becomes symmetric when linear fingertip forces are applied, (4) is symmetrically rearranged as:

$$[\boldsymbol{K}_{\mathrm{o}}] = \left[\boldsymbol{K}'_{\mathrm{o}}\right] + \left([T_{\mathrm{f}}]^{\mathrm{T}} \circ \left[\boldsymbol{H}_{\mathrm{oo}}^{\mathrm{f}}\right]\right) = \left[\boldsymbol{G}_{\mathrm{o}}^{\mathrm{f}}\right]^{\mathrm{T}} [\boldsymbol{K}_{\mathrm{f}}] \left[\boldsymbol{G}_{\mathrm{o}}^{\mathrm{f}}\right]. \tag{5}$$

In a common robot hand system, inter-finger coupling exists. If the inter-finger coupling can be eliminated, each finger can be independently controlled, which makes the hand control relatively easy. Recently, an independent finger and independent joint-based compliance control was proposed [11]. The paper showed that the desired compliance characteristics in the operational space can be achievable by controlling the independent compliance characteristic of each finger. For more explanation, we illustrate a compliance control example of using a two-fingered robot hand. Let the desired 2×2 object stiffness matrix in the operational

space of the hand be given as:

$$[\boldsymbol{K}_{\mathrm{o}}] = \begin{bmatrix} \boldsymbol{K}_{\mathrm{o}xx} & \boldsymbol{K}_{\mathrm{o}xy} \\ \boldsymbol{K}_{\mathrm{o}yx} & \boldsymbol{K}_{\mathrm{o}yy} \end{bmatrix}, \tag{6}$$

and the 4×4 stiffness matrix in the fingertip space is generally represented by:

$$[\boldsymbol{K}_{\mathrm{f}}] = \left[\begin{array}{cc|cc} {}^{1}\boldsymbol{K}_{\mathrm{f}xx} & {}^{1}\boldsymbol{K}_{\mathrm{f}xy} & {}^{12}\boldsymbol{K}_{\mathrm{f}xx} & {}^{12}\boldsymbol{K}_{\mathrm{f}xy} \\ {}^{1}\boldsymbol{K}_{\mathrm{f}yx} & {}^{1}\boldsymbol{K}_{\mathrm{f}yy} & {}^{12}\boldsymbol{K}_{\mathrm{f}yx} & {}^{12}\boldsymbol{K}_{\mathrm{f}yy} \\ \hline {}^{21}\boldsymbol{K}_{\mathrm{f}xx} & {}^{21}\boldsymbol{K}_{\mathrm{f}xy} & {}^{2}\boldsymbol{K}_{\mathrm{f}xx} & {}^{2}\boldsymbol{K}_{\mathrm{f}xy} \\ {}^{21}\boldsymbol{K}_{\mathrm{f}yx} & {}^{21}\boldsymbol{K}_{\mathrm{f}yy} & {}^{2}\boldsymbol{K}_{\mathrm{f}yx} & {}^{2}\boldsymbol{K}_{\mathrm{f}yy} \end{array}\right], \tag{7}$$

where the off-diagonal blocks denote the inter-finger coupling matrices, and ${}^{i}\boldsymbol{K}_{\mathrm{f}xy}$ ($i = 1, 2$) denotes the coupling stiffness elements between the x- and y-direction in the ith fingertip space.

Also, a grip Jacobian matrix relating the small displacement of the operational position to those of the finger positions is given by:

$$\begin{bmatrix} {}^{1}\boldsymbol{G}_{\mathrm{o}}^{\mathrm{f}} \\ {}^{2}\boldsymbol{G}_{\mathrm{o}}^{\mathrm{f}} \end{bmatrix} = \begin{bmatrix} b_{11} & b_{12} \\ b_{21} & b_{22} \\ b_{31} & b_{32} \\ b_{41} & b_{42} \end{bmatrix}. \tag{8}$$

Here, our objective is to eliminate inter-finger couplings, as well as the coupling of the fingertip space, for effective hybrid control in the fingertip space. Thus, the stiffness matrix satisfying this objective is set up as:

$$[\boldsymbol{K}_{\mathrm{f}}^{\mathrm{d}}] = \left[\begin{array}{cc|cc} {}^{1}\boldsymbol{K}_{\mathrm{f}xx}^{\mathrm{d}} & 0 & 0 & 0 \\ 0 & {}^{1}\boldsymbol{K}_{\mathrm{f}yy}^{\mathrm{d}} & 0 & 0 \\ \hline 0 & 0 & {}^{2}\boldsymbol{K}_{\mathrm{f}xx}^{\mathrm{d}} & 0 \\ 0 & 0 & 0 & {}^{2}\boldsymbol{K}_{\mathrm{f}yy}^{\mathrm{d}} \end{array}\right], \tag{9}$$

where ${}^{i}\boldsymbol{K}_{\mathrm{f}xx}^{\mathrm{d}}$ and ${}^{i}\boldsymbol{K}_{\mathrm{f}yy}^{\mathrm{d}}$ denote the desired x- and y-directional stiffness elements in the fingertip space of the ith finger, respectively.

Then, (6) can be rearranged as a vector form:

$$K_{\mathrm{oo}} = \left[\boldsymbol{B}_{\mathrm{f}}^{\mathrm{o}}\right] K_{\mathrm{ff}}, \tag{10}$$

where:

$$K_{\mathrm{oo}} = [\, \boldsymbol{K}_{\mathrm{o}xx} \quad \boldsymbol{K}_{\mathrm{o}xy} \quad \boldsymbol{K}_{\mathrm{o}yy} \,]^{\mathrm{T}},$$
$$K_{\mathrm{ff}} = \left[\, {}^{1}\boldsymbol{K}_{\mathrm{f}xx}^{\mathrm{d}} \quad {}^{1}\boldsymbol{K}_{\mathrm{f}yy}^{\mathrm{d}} \quad {}^{2}\boldsymbol{K}_{\mathrm{f}xx}^{\mathrm{d}} \quad {}^{2}\boldsymbol{K}_{\mathrm{f}yy}^{\mathrm{d}} \,\right]^{\mathrm{T}},$$

and:

$$[\boldsymbol{B}_{\mathrm{f}}^{\mathrm{o}}] = \begin{bmatrix} (b_{11})^2 & (b_{21})^2 & (b_{31})^2 & (b_{41})^2 \\ b_{11}b_{12} & b_{21}b_{22} & b_{31}b_{32} & b_{41}b_{42} \\ (b_{12})^2 & (b_{22})^2 & (b_{32})^2 & (b_{42})^2 \end{bmatrix}.$$

In (10), K_{oo} and K_{ff} denote the independent stiffness elements of the operational space and the fingertip space, respectively. $[\boldsymbol{B}_f^o]$ denotes the stiffness mapping matrix relating the operational space to the fingertip space and the elements of $[\boldsymbol{B}_f^o]$ are dependent on the grasp geometry. To be specific, the sign of some elements of $[\boldsymbol{B}_f^o]$ may be changed from positive to negative or zero. Accordingly, a change in the values of operational stiffness elements should be considerably observed and, thus, operational stiffness elements should be considerably specified in consideration of the grasp geometry.

Generally, the stiffness relation between the operational space and the fingertip space given in (5) can be expressed by:

$$\begin{bmatrix} \boldsymbol{K}_{ox} & \boldsymbol{K}_{oxy} & \boldsymbol{K}_{oxz} & \boldsymbol{K}_{ox\gamma} & \boldsymbol{K}_{ox\beta} & \boldsymbol{K}_{ox\alpha} \\ \boldsymbol{K}_{oyx} & \boldsymbol{K}_{oy} & \boldsymbol{K}_{oyz} & \boldsymbol{K}_{oy\gamma} & \boldsymbol{K}_{oy\beta} & \boldsymbol{K}_{oy\alpha} \\ \boldsymbol{K}_{ozx} & \boldsymbol{K}_{ozy} & \boldsymbol{K}_{oz} & \boldsymbol{K}_{oz\gamma} & \boldsymbol{K}_{oz\beta} & \boldsymbol{K}_{oz\alpha} \\ \boldsymbol{K}_{o\gamma x} & \boldsymbol{K}_{o\gamma y} & \boldsymbol{K}_{o\gamma z} & \boldsymbol{K}_{o\gamma} & \boldsymbol{K}_{o\gamma\beta} & \boldsymbol{K}_{o\gamma\alpha} \\ \boldsymbol{K}_{o\beta x} & \boldsymbol{K}_{o\beta y} & \boldsymbol{K}_{o\beta z} & \boldsymbol{K}_{o\beta\gamma} & \boldsymbol{K}_{o\beta} & \boldsymbol{K}_{o\beta\alpha} \\ \boldsymbol{K}_{o\alpha x} & \boldsymbol{K}_{o\alpha y} & \boldsymbol{K}_{o\alpha z} & \boldsymbol{K}_{o\alpha\gamma} & \boldsymbol{K}_{o\alpha\beta} & \boldsymbol{K}_{o\alpha} \end{bmatrix} = \begin{bmatrix} g_{11} & g_{1j} & \cdots & g_{16} \\ g_{k1} & g_{kj} & \cdots & g_{k6} \\ \vdots & \vdots & \ddots & \vdots \\ g_{m1} & g_{mj} & \cdots & g_{m6} \end{bmatrix}^{\mathrm{T}}$$

$$\times \begin{bmatrix} {}^{1}\boldsymbol{K}_f & {}^{12}\boldsymbol{K}_f & \cdots & {}^{1n_f}\boldsymbol{K}_f \\ {}^{21}\boldsymbol{K}_f & {}^{2}\boldsymbol{K}_f & \cdots & {}^{2n_f}\boldsymbol{K}_f \\ \vdots & \vdots & \ddots & \vdots \\ {}^{n_f1}\boldsymbol{K}_f & {}^{n_f2}\boldsymbol{K}_f & \cdots & {}^{n_f}\boldsymbol{K}_f \end{bmatrix} \begin{bmatrix} g_{11} & g_{1j} & \cdots & g_{16} \\ g_{k1} & g_{kj} & \cdots & g_{k6} \\ \vdots & \vdots & \ddots & \vdots \\ g_{m1} & g_{mj} & \cdots & g_{m6} \end{bmatrix}, \tag{11}$$

where subscripts γ, β and α imply the rotational angles about x-, y- and z-axis, respectively. The element g_{kj} $(j = 2, \ldots, 5,\ k = 2, \ldots, m-1)$ denotes the kj-element of $[\boldsymbol{G}_o^f]$ presented in (1) and thus it depends on the grasp geometry.

If all elements except the diagonal elements of the fingertip space in (11) are zero, an independent finger-based control can be implemented. Similarly, the independent stiffness relation between the operational space and the fingertip space can be described as (10) [11].

Consequently, by solving the linear programming problem given by (10) subject to $K_{ff} \geqslant 0$, the desired compliance characteristics in the operational space can be independently distributed to the fingertip space and thus the operational compliance characteristics can be achievable by controlling the independent compliance characteristic of each finger. The advantage of the alternative form given by (10) is that, first, it enables one to analyze the stiffness geometry and, second, it is computationally efficient in comparison to the original relation given by (5).

3. COMPLIANCE PLANNING FOR ASSEMBLY TASKS

Historically, for assembly tasks, passive RCC devices [8] and active accommodation [13, 22] have been popularly employed in real implementations. However, both methodologies were mostly applied to a single robot manipulator. This section will treat an assembly task using multi-fingered hands. Specifically, a guideline

to specify the compliance center in the operational space is provided through planar and 3D assembly tasks manipulated by three-fingered hands.

3.1. Planar assembly tasks

3.1.1. Straight peg. When an object is assembled by multi-fingered hands as shown in Fig. 2, the performance of the given task is closely related to the grasp geometry and the location of the compliance center [14, 25]. Consider the compliance center lying in the point $\boldsymbol{O}_1$ of Fig. 2. The independent stiffness relation between the operational space and the fingertip space can be expressed as:

$$K_{\mathrm{oo}} = \left[\boldsymbol{B}_{\mathrm{f}}^{\mathrm{o}}\right] K_{\mathrm{ff}} = \begin{bmatrix} 1 & 0 & 1 & 0 & 1 & 0 \\ 0 & 0 & 0 & 0 & 0 & 0 \\ -y_1 & 0 & -y_2 & 0 & y_3 & 0 \\ 0 & 1 & 0 & 1 & 0 & 1 \\ 0 & -x_1 & 0 & x_2 & 0 & x_3 \\ y_1^2 & x_1^2 & y_2^2 & x_2^2 & y_3^2 & x_3^2 \end{bmatrix} K_{\mathrm{ff}}, \tag{12}$$

where:

$$K_{\mathrm{oo}} = [\boldsymbol{K}_{\mathrm{o}xx}\ \boldsymbol{K}_{\mathrm{o}xy}\ \boldsymbol{K}_{\mathrm{o}x\phi}\ \boldsymbol{K}_{\mathrm{o}yy}\ \boldsymbol{K}_{\mathrm{o}y\phi}\ \boldsymbol{K}_{\mathrm{o}\phi\phi}]^{\mathrm{T}},$$

and:

$$K_{\mathrm{ff}} = \left[{}^{1}\boldsymbol{K}_{\mathrm{f}xx}\ {}^{1}\boldsymbol{K}_{\mathrm{f}yy}\ {}^{2}\boldsymbol{K}_{\mathrm{f}xx}\ {}^{2}\boldsymbol{K}_{\mathrm{f}yy}\ {}^{3}\boldsymbol{K}_{\mathrm{f}xx}\ {}^{3}\boldsymbol{K}_{\mathrm{f}yy}\right]^{\mathrm{T}}.$$

Also, x_i and y_i denote the elements of the position vectors directing from the ith finger contact position to the task position, and they are given to be all positive.

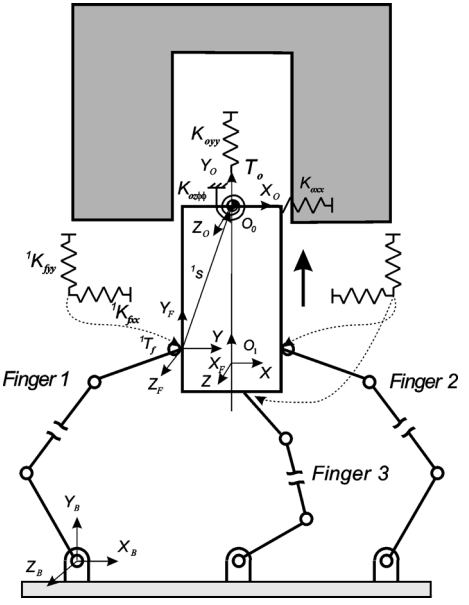

Figure 2. A straight peg-in-hole task using a three-fingered robotic hand.

${}^{i}\boldsymbol{K}_{\mathrm{f}xx}$ and ${}^{i}\boldsymbol{K}_{\mathrm{f}yy}$ represent the x- and y-directional stiffness elements in the fingertip space of the ith finger, respectively.

Note that the elements of the second row of the mapping matrix $[\boldsymbol{B}_{\mathrm{f}}^{\mathrm{o}}]$ in (12) are calculated as zero. This is because we excluded the coupling terms ${}^{i}\boldsymbol{K}_{\mathrm{f}xy}$ ($i = 1, 2, 3$) in the fingertip space for independent compliance control. Thus, we have zero $\boldsymbol{K}_{\mathrm{o}xy}$, which, in fact, is a linear combination of ${}^{i}\boldsymbol{K}_{\mathrm{f}xy}$ ($i = 1, 2, 3$).

Thus, the resultant stiffness matrix in the operational space can be specified as follows:

$$\begin{bmatrix} \boldsymbol{K}_{\mathrm{o}xx} & \boldsymbol{K}_{\mathrm{o}xy} & \boldsymbol{K}_{\mathrm{o}x\phi} \\ \boldsymbol{K}_{\mathrm{o}yx} & \boldsymbol{K}_{\mathrm{o}yy} & \boldsymbol{K}_{\mathrm{o}y\phi} \\ \boldsymbol{K}_{\mathrm{o}\phi x} & \boldsymbol{K}_{\mathrm{o}\phi y} & \boldsymbol{K}_{\mathrm{o}\phi\phi} \end{bmatrix} = \begin{bmatrix} S & 0 & 0, \pm\psi_1 \\ 0 & L & 0, \pm\psi_2 \\ 0, \pm\psi_1 & 0, \pm\psi_2 & S \end{bmatrix}, \tag{13}$$

where ψ_1 and ψ_2 are all positive parameters. S and L mean small and large values of stiffness, respectively. The diagonal elements can be determined by considering the task characteristics for each direction [12–14]. Coupling components, ψ_1 and ψ_2, can be arbitrarily determined and also those parameters can be suitably adjusted by considering additional control performance (e.g. the jamming effect of assembly tasks [15]). Among the elements of the matrix given by (13), $0, \pm\psi_1$ implies that it could be designed as 0, or $\pm\psi_1$.

In the case where the compliance center is assigned at the point $\boldsymbol{O}_0$ of Fig. 2, the signs of y_1 and y_2 in the third row of $[\boldsymbol{B}_{\mathrm{f}}^{\mathrm{o}}]$ are changed by moving the compliance center from $\boldsymbol{O}_1$ to $\boldsymbol{O}_0$. Thus, the stiffness matrix in the operational space should be differently specified as follows:

$$\begin{bmatrix} \boldsymbol{K}_{\mathrm{o}xx} & \boldsymbol{K}_{\mathrm{o}xy} & \boldsymbol{K}_{\mathrm{o}x\phi} \\ \boldsymbol{K}_{\mathrm{o}yx} & \boldsymbol{K}_{\mathrm{o}yy} & \boldsymbol{K}_{\mathrm{o}y\phi} \\ \boldsymbol{K}_{\mathrm{o}\phi x} & \boldsymbol{K}_{\mathrm{o}\phi y} & \boldsymbol{K}_{\mathrm{o}\phi\phi} \end{bmatrix} = \begin{bmatrix} S & 0 & +\psi_1 \\ 0 & L & 0, \pm\psi_2 \\ +\psi_1 & 0, \pm\psi_2 & S \end{bmatrix}. \tag{14}$$

In this case, the stiffness element $\boldsymbol{K}_{\mathrm{o}x\phi}$ relating the x-direction to the ϕ-direction always turns out as a positive value. Existence of the off-diagonal term sometimes causes kinematic coupling among control directions, which is undesirable or desirable according to the purpose of the given task. Also, in this case, a small disturbance in the x-direction due to a collision between the peg and the wall would cause a counter-clockwise rotational motion of the peg, which might cause a jamming of the peg inside the hole. Thus, the stiffness characteristic given by (12), which is completely decoupled, would be desirable for this application. On the other hand, when the left-side of the peg in Fig. 2 is being contacted on the hole, the insertion task may be easily achieved because the inserted peg will rotate to the counter-clockwise direction by assigning a positive ψ_1 [26].

3.1.2. L-type peg. In assembly tasks, the types of pegs being pegged are diverse. Initially, we consider that a multi-fingered hand inserts a left-angled peg into a hole as shown in Fig. 3a.

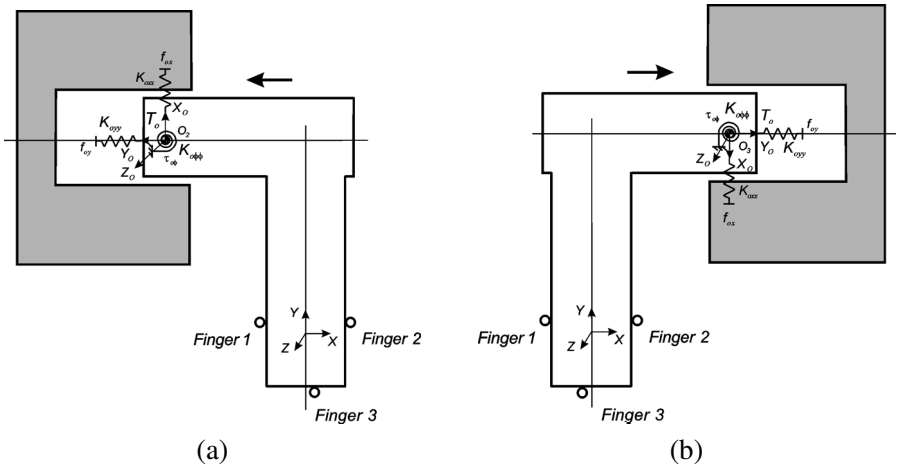

(a) (b)

Figure 3. Peg-in-hole tasks using a three-fingered robotic hand. (a) Left-angled peg. (b) Right-angled peg.

The stiffness mapping matrix, $[\boldsymbol{B}_{\mathrm{f}}^{\mathrm{o}}]$, of (10) is given by

$$[\boldsymbol{B}_{\mathrm{f}}^{\mathrm{o}}] = \begin{bmatrix} 0 & 1 & 0 & 1 & 0 & 1 \\ 0 & 0 & 0 & 0 & 0 & 0 \\ 0 & -x_1 & 0 & -x_2 & 0 & -x_3 \\ 1 & 0 & 1 & 0 & 1 & 0 \\ -y_1 & 0 & -y_2 & 0 & -y_3 & 0 \\ y_1^2 & x_1^2 & y_2^2 & x_2^2 & y_3^2 & x_3^2 \end{bmatrix}. \tag{15}$$

The third and fifth rows of $[\boldsymbol{B}_{\mathrm{f}}^{\mathrm{o}}]$ in (15) have zero or minus signs, since the three influence coefficients (i.e. x_i, y_i, $(i = 1, 2, 3)$) are always positive. Therefore, we can easily notice that the signs of $\boldsymbol{K}_{\mathrm{o}x\phi}$ and $\boldsymbol{K}_{\mathrm{o}y\phi}$ corresponding to the third and fifth rows of $[\boldsymbol{B}_{\mathrm{f}}^{\mathrm{o}}]$ are always negative. Thus, the stiffness matrix in the operational space can be specified as follows:

$$\begin{bmatrix} \boldsymbol{K}_{\mathrm{o}xx} & \boldsymbol{K}_{\mathrm{o}xy} & \boldsymbol{K}_{\mathrm{o}x\phi} \\ \boldsymbol{K}_{\mathrm{o}yx} & \boldsymbol{K}_{\mathrm{o}yy} & \boldsymbol{K}_{\mathrm{o}y\phi} \\ \boldsymbol{K}_{\mathrm{o}\phi x} & \boldsymbol{K}_{\mathrm{o}\phi y} & \boldsymbol{K}_{\mathrm{o}\phi\phi} \end{bmatrix} = \begin{bmatrix} S & 0 & -\psi_1 \\ 0 & L & -\psi_2 \\ -\psi_1 & -\psi_2 & S \end{bmatrix}. \tag{16}$$

For independent task-space control, it is desirable to have a diagonal operational stiffness matrix. However, the grasping geometry of Fig. 3a does not allow this objective since $\boldsymbol{K}_{\mathrm{o}x\phi}$ and $\boldsymbol{K}_{\mathrm{o}y\phi}$ are given negative values. That is, the signs of $\boldsymbol{K}_{\mathrm{o}x\phi}$ and $\boldsymbol{K}_{\mathrm{o}y\phi}$ are not controllable in this grasp configuration. In this case, they are determined by the following procedures.

Next, consider that a multi-fingered hand inserts a right-angled peg into a hole as shown in Fig. 3b. The stiffness mapping matrix of $[\boldsymbol{B}_{\mathrm{f}}^{\mathrm{o}}]$ between the operational space and the fingertip space is given by:

$$\left[\boldsymbol{B}_{\mathrm{f}}^{\mathrm{o}}\right] = \begin{bmatrix} 0 & 1 & 0 & 1 & 0 & 1 \\ 0 & 0 & 0 & 0 & 0 & 0 \\ 0 & -x_1 & 0 & -x_2 & 0 & -x_3 \\ 1 & 0 & 1 & 0 & 1 & 0 \\ y_1 & 0 & y_2 & 0 & y_3 & 0 \\ y_1^2 & x_1^2 & y_2^2 & x_2^2 & y_3^2 & x_3^2 \end{bmatrix}. \tag{17}$$

Here, the fifth rows of $[\boldsymbol{B}_{\mathrm{f}}^{\mathrm{o}}]$ have all positive signs opposite to the case of a left-angled peg-in-hole task. Thus, $\boldsymbol{K}_{\mathrm{o}y\phi}$ corresponding to the fifth row of $[\boldsymbol{B}_{\mathrm{f}}^{\mathrm{o}}]$ is always a positive value and the stiffness matrix in the operational space can be specified as follows:

$$\begin{bmatrix} \boldsymbol{K}_{\mathrm{o}xx} & \boldsymbol{K}_{\mathrm{o}xy} & \boldsymbol{K}_{\mathrm{o}x\phi} \\ \boldsymbol{K}_{\mathrm{o}yx} & \boldsymbol{K}_{\mathrm{o}yy} & \boldsymbol{K}_{\mathrm{o}y\phi} \\ \boldsymbol{K}_{\mathrm{o}\phi x} & \boldsymbol{K}_{\mathrm{o}\phi y} & \boldsymbol{K}_{\mathrm{o}\phi\phi} \end{bmatrix} = \begin{bmatrix} S & 0 & -\psi_1 \\ 0 & L & +\psi_2 \\ -\psi_1 & +\psi_2 & S \end{bmatrix}. \tag{18}$$

3.1.3. T-type peg. This section considers that a T-typed peg is inserted into a hole by using two multi-fingered hands as shown in Fig. 4. In this case, the stiffness matrix in the operational space by referring to (5) can be expressed as

$$[\boldsymbol{K}_{\mathrm{o}}] = \sum_{i=1}^{2} {}^{i}\left[\boldsymbol{G}_{\mathrm{o}}^{\mathrm{f}}\right]^{\mathrm{T}} {}^{i}[\boldsymbol{K}_{\mathrm{f}}] \, {}^{i}\left[\boldsymbol{G}_{\mathrm{o}}^{\mathrm{f}}\right], \tag{19}$$

where ${}^{i}[\boldsymbol{K}_{\mathrm{f}}]$ and ${}^{i}[\boldsymbol{G}_{\mathrm{o}}^{\mathrm{f}}]$ denote the stiffness matrix in the fingertip space of the ith hand and the Jacobian matrix relating the fingertip space of the ith hand to the operational space, respectively. Also, the independent stiffness mapping matrix between the operational space and the fingertip space of the two-handed assembling system can be represented by:

$$[\boldsymbol{B}_{\mathrm{f}}^{\mathrm{o}}] = \left[{}^{1}\left[\boldsymbol{B}_{\mathrm{f}}^{\mathrm{o}}\right] {}^{2}\left[\boldsymbol{B}_{\mathrm{f}}^{\mathrm{o}}\right]\right], \tag{20}$$

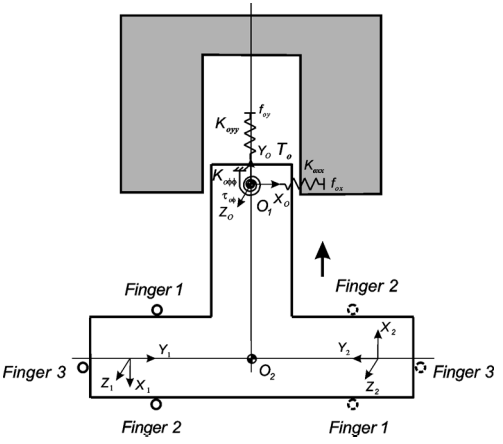

Figure 4. A perpendicular peg-in-hole task using two hands.

where ${}^{i}[\boldsymbol{B}_{\mathrm{f}}^{\mathrm{o}}]$ denotes the stiffness mapping matrix between the operational space and the fingertip space of the ith hand.

When each hand grasps the peg for the compliance center $\boldsymbol{O}_1$ of Fig. 4, this is identical to the combination of the two cases of Fig. 3a and b. As a result, the coupling stiffness element $\boldsymbol{K}_{\mathrm{o}y\phi}$ can be arbitrarily specified, but $\boldsymbol{K}_{\mathrm{o}x\phi}$ cannot be arbitrarily planned. If the compliance center is moved to the point $\boldsymbol{O}_2$, the sign of the kinematic influence coefficient y_1 in (15) changes into negative and the sign of the kinematic influence coefficient y_2 in (17) changes into negative. Thus, we can notice that the coupling stiffness element $\boldsymbol{K}_{\mathrm{o}y\phi}$ is arbitrarily specified, but $\boldsymbol{K}_{\mathrm{o}x\phi}$ still cannot be arbitrarily planned and, specifically, $\boldsymbol{K}_{\mathrm{o}x\phi}$ is always negative.

3.2. 3D assembly tasks

3.2.1. L-type peg. When a multi-fingered hand assembles a straight peg into a hole in a 3D space, the stiffness matrix to be specified in the operational space was analyzed based on the grasp geometry [16]. According to the analysis, it is possible that the 6-d.o.f. compliance control can be achievable with a five-fingered hand. In order to specify the operational compliance characteristic in the 3D space, we first investigate the stiffness relation between the operational space and the fingertip space for the left-angled peg model of Fig. 5a. It is given by:

$$K_{\mathrm{oo}} = \left[\boldsymbol{B}_{\mathrm{f}}^{\mathrm{o}}\right] K_{ff}$$

$$\begin{bmatrix} \boldsymbol{K}_{\mathrm{o}xx} \\ \boldsymbol{K}_{\mathrm{o}xy} \\ \boldsymbol{K}_{\mathrm{o}xz} \\ \boldsymbol{K}_{\mathrm{o}x\gamma} \\ \boldsymbol{K}_{\mathrm{o}x\beta} \\ \boldsymbol{K}_{\mathrm{o}x\alpha} \\ \boldsymbol{K}_{\mathrm{o}yy} \\ \boldsymbol{K}_{\mathrm{o}yz} \\ \boldsymbol{K}_{\mathrm{o}y\gamma} \\ \boldsymbol{K}_{\mathrm{o}y\beta} \\ \boldsymbol{K}_{\mathrm{o}y\alpha} \\ \boldsymbol{K}_{\mathrm{o}zz} \\ \boldsymbol{K}_{\mathrm{o}z\gamma} \\ \boldsymbol{K}_{\mathrm{o}z\beta} \\ \boldsymbol{K}_{\mathrm{o}z\alpha} \\ \boldsymbol{K}_{\mathrm{o}\gamma\gamma} \\ \boldsymbol{K}_{\mathrm{o}\gamma\beta} \\ \boldsymbol{K}_{\mathrm{o}\gamma\alpha} \\ \boldsymbol{K}_{\mathrm{o}\beta\beta} \\ \boldsymbol{K}_{\mathrm{o}\beta\alpha} \\ \boldsymbol{K}_{\mathrm{o}\alpha\alpha} \end{bmatrix} = \begin{bmatrix} 0 & 0 & 1 & 0 & 0 & 1 & 0 & 0 & 1 & 0 & 0 & 1 & 0 & 0 & 1 \\ 0 & 0 & 0 & 0 & 0 & 0 & 0 & 0 & 0 & 0 & 0 & 0 & 0 & 0 & 0 \\ 0 & 0 & 0 & 0 & 0 & 0 & 0 & 0 & 0 & 0 & 0 & 0 & 0 & 0 & 0 \\ 0 & 0 & 0 & 0 & 0 & 0 & 0 & 0 & 0 & 0 & 0 & 0 & 0 & 0 & 0 \\ 0 & 0 & x_1 & 0 & 0 & x_2 & 0 & 0 & x_3 & 0 & 0 & x_4 & 0 & 0 & x_5 \\ \hline 0 & 0 & -y_1 & 0 & 0 & y_2 & 0 & 0 & -y_3 & 0 & 0 & y_4 & 0 & 0 & -y_5 \\ 0 & 1 & 0 & 0 & 1 & 0 & 0 & 1 & 0 & 0 & 1 & 0 & 0 & 1 & 0 \\ 0 & 0 & 0 & 0 & 0 & 0 & 0 & 0 & 0 & 0 & 0 & 0 & 0 & 0 & 0 \\ 0 & -x_1 & 0 & 0 & -x_2 & 0 & 0 & -x_3 & 0 & 0 & -x_4 & 0 & 0 & -x_5 & 0 \\ \hline 0 & 0 & 0 & 0 & 0 & 0 & 0 & 0 & 0 & 0 & 0 & 0 & 0 & 0 & 0 \\ 0 & -z_1 & 0 & 0 & -z_2 & 0 & 0 & -z_3 & 0 & 0 & -z_4 & 0 & 0 & -z_5 & 0 \\ \hline 1 & 0 & 0 & 1 & 0 & 0 & 1 & 0 & 0 & 1 & 0 & 0 & 1 & 0 & 0 \\ y_1 & 0 & 0 & -y_2 & 0 & 0 & y_3 & 0 & 0 & -y_4 & 0 & 0 & y_5 & 0 & 0 \\ z_1 & 0 & 0 & z_2 & 0 & 0 & z_3 & 0 & 0 & z_4 & 0 & 0 & z_5 & 0 & 0 \\ \hline 0 & 0 & 0 & 0 & 0 & 0 & 0 & 0 & 0 & 0 & 0 & 0 & 0 & 0 & 0 \\ y_1^2 & x_1^2 & 0 & y_2^2 & x_2^2 & 0 & y_3^2 & x_3^2 & 0 & y_4^2 & x_4^2 & 0 & y_5^2 & 0 & x_5^2 \\ y_1 z_1 & 0 & 0 & -y_2 z_2 & 0 & 0 & y_3 z_3 & 0 & 0 & -y_4 z_4 & 0 & 0 & y_5 z_5 & 0 & 0 \\ 0 & x_1 z_1 & 0 & 0 & x_2 z_2 & 0 & 0 & x_3 z_3 & 0 & 0 & x_4 z_4 & 0 & 0 & x_5 z_5 & 0 \\ \hline z_1^2 & 0 & x_1^2 & z_2^2 & 0 & x_2^2 & z_3^2 & 0 & x_3^2 & z_4^2 & 0 & x_4^2 & z_5^2 & 0 & x_5^2 \\ 0 & 0 & -x_1 y_1 & 0 & 0 & x_2 y_2 & 0 & 0 & -x_3 y_3 & 0 & 0 & x_4 y_4 & 0 & 0 & -x_5 y_5 \\ 0 & z_1^2 & y_1^2 & 0 & z_2^2 & y_2^2 & 0 & z_3^2 & y_3^2 & 0 & z_4^2 & y_4^2 & 0 & z_5^2 & y_5^2 \end{bmatrix}$$

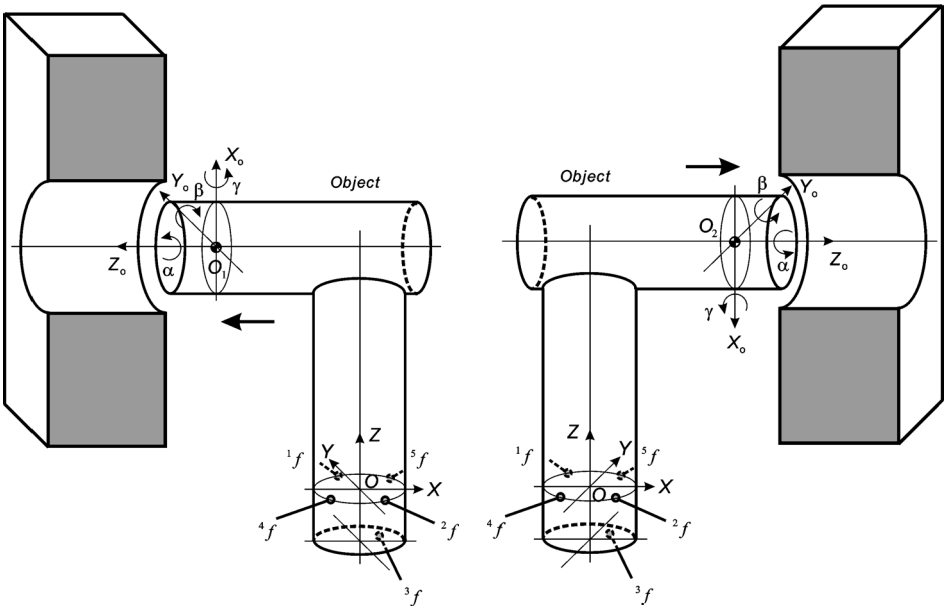

Figure 5. Peg-in-hole tasks using a five-fingered hand in 3D space. (a) Left-angled peg. (b) Right-angled peg.

$$\times \begin{bmatrix} {}^{1}\boldsymbol{K}_{\mathrm{f}xx} \\ {}^{1}\boldsymbol{K}_{\mathrm{f}yy} \\ {}^{1}\boldsymbol{K}_{\mathrm{f}zz} \\ {}^{2}\boldsymbol{K}_{\mathrm{f}xx} \\ {}^{2}\boldsymbol{K}_{\mathrm{f}yy} \\ {}^{2}\boldsymbol{K}_{\mathrm{f}zz} \\ {}^{3}\boldsymbol{K}_{\mathrm{f}xx} \\ {}^{3}\boldsymbol{K}_{\mathrm{f}yy} \\ {}^{3}\boldsymbol{K}_{\mathrm{f}zz} \\ {}^{4}\boldsymbol{K}_{\mathrm{f}xx} \\ {}^{4}\boldsymbol{K}_{\mathrm{f}yy} \\ {}^{4}\boldsymbol{K}_{\mathrm{f}zz} \\ {}^{5}\boldsymbol{K}_{\mathrm{f}xx} \\ {}^{5}\boldsymbol{K}_{\mathrm{f}yy} \\ {}^{5}\boldsymbol{K}_{\mathrm{f}zz} \end{bmatrix}, \tag{21}$$

where $\boldsymbol{K}_{\mathrm{o}ii}$ and $\boldsymbol{K}_{\mathrm{o}ij}$ denote the i-directional stiffness element and the coupling stiffness element existing between the i- and j-directions, respectively, and γ, β and α subscripts denote the rotational directions for x-, y- and z-directions, respectively. Also x_i, y_i, and z_i denote the elements of position vectors directing from the ith finger contact position to the task position, and they are given all positive. ${}^{i}\boldsymbol{K}_{\mathrm{f}xx}$,

${}^{i}\boldsymbol{K}_{\mathrm{f}yy}$ and ${}^{i}\boldsymbol{K}_{\mathrm{f}zz}$ represent the x-, y- and z-directional stiffness elements in the fingertip space of the ith finger, respectively.

In (21), all elements of $[\boldsymbol{B}_{\mathrm{f}}^{\mathrm{o}}]_5$, $[\boldsymbol{B}_{\mathrm{f}}^{\mathrm{o}}]_9$, $[\boldsymbol{B}_{\mathrm{f}}^{\mathrm{o}}]_{11}$, $[\boldsymbol{B}_{\mathrm{f}}^{\mathrm{o}}]_{14}$ and $[\boldsymbol{B}_{\mathrm{f}}^{\mathrm{o}}]_{18}$ have the same signs, respectively, where $[\boldsymbol{B}_{\mathrm{f}}^{\mathrm{o}}]_i$ denotes the ith row of $[\boldsymbol{B}_{\mathrm{f}}^{\mathrm{o}}]$. Therefore, the stiffness elements $\boldsymbol{K}_{\mathrm{o}x\beta}$, $\boldsymbol{K}_{\mathrm{o}y\gamma}$, $\boldsymbol{K}_{\mathrm{o}y\alpha}$, $\boldsymbol{K}_{z\beta}$ and $\boldsymbol{K}_{\mathrm{o}\gamma\alpha}$ cannot be arbitrarily planned.

Consequently, the stiffness matrix in the operational space can be specified as follows:

$$\begin{bmatrix} \boldsymbol{K}_{\mathrm{o}xx} & \boldsymbol{K}_{\mathrm{o}xy} & \boldsymbol{K}_{\mathrm{o}xz} & \boldsymbol{K}_{\mathrm{o}x\gamma} & \boldsymbol{K}_{\mathrm{o}x\beta} & \boldsymbol{K}_{\mathrm{o}x\alpha} \\ \boldsymbol{K}_{\mathrm{o}yx} & \boldsymbol{K}_{\mathrm{o}yy} & \boldsymbol{K}_{\mathrm{o}yz} & \boldsymbol{K}_{\mathrm{o}y\gamma} & \boldsymbol{K}_{\mathrm{o}y\beta} & \boldsymbol{K}_{\mathrm{o}y\alpha} \\ \boldsymbol{K}_{\mathrm{o}zx} & \boldsymbol{K}_{\mathrm{o}zy} & \boldsymbol{K}_{\mathrm{o}zz} & \boldsymbol{K}_{\mathrm{o}z\gamma} & \boldsymbol{K}_{\mathrm{o}z\beta} & \boldsymbol{K}_{\mathrm{o}z\alpha} \\ \boldsymbol{K}_{\mathrm{o}\gamma x} & \boldsymbol{K}_{\mathrm{o}\gamma y} & \boldsymbol{K}_{\mathrm{o}\gamma z} & \boldsymbol{K}_{\mathrm{o}\gamma\gamma} & \boldsymbol{K}_{\mathrm{o}\gamma\beta} & \boldsymbol{K}_{\mathrm{o}\gamma\alpha} \\ \boldsymbol{K}_{\mathrm{o}\beta x} & \boldsymbol{K}_{\mathrm{o}\beta y} & \boldsymbol{K}_{\mathrm{o}\beta z} & \boldsymbol{K}_{\mathrm{o}\beta\gamma} & \boldsymbol{K}_{\mathrm{o}\beta\beta} & \boldsymbol{K}_{\mathrm{o}\beta\alpha} \\ \boldsymbol{K}_{\mathrm{o}\alpha x} & \boldsymbol{K}_{\mathrm{o}\alpha y} & \boldsymbol{K}_{\mathrm{o}\alpha z} & \boldsymbol{K}_{\mathrm{o}\alpha\gamma} & \boldsymbol{K}_{\mathrm{o}\alpha\beta} & \boldsymbol{K}_{\mathrm{o}\alpha\alpha} \end{bmatrix}$$

$$= \begin{bmatrix} S & 0 & 0 & 0 & +\psi_1 & 0, \pm\psi_2 \\ 0 & S & 0 & -\psi_3 & 0 & -\psi_4 \\ 0 & 0 & L & 0, \pm\psi_5 & +\psi_6 & 0 \\ 0 & -\psi_3 & 0, \pm\psi_5 & S & 0, \pm\psi_7 & +\psi_8 \\ +\psi_1 & 0 & +\psi_6 & 0, \pm\psi_7 & S & 0, \pm\psi_9 \\ 0, \pm\psi_2 & -\psi_4 & 0 & +\psi_8 & 0, \pm\psi_9 & L \end{bmatrix}, \tag{22}$$

where ψ_i $(i = 1, 2, \ldots, 9)$ are all positive parameters. S and L imply small and large values of stiffness, respectively. The diagonal elements are determined according to the task requirements [12–14].

In (22), ψ_i $(i = 2, 5, 7, 9)$ can be arbitrarily determined and also those parameters can be suitably adjusted by considering additional control performance (e.g. the jamming effect of assembly tasks). On the other hand, ψ_j $(j = 1, 3, 4, 6, 8)$ cannot be arbitrarily planned, but can be determined by the procedure presented in Ref. [25].

Now, consider that a multi-fingered hand inserts a right-angled peg into a hole as shown in Fig. 5b. In this case, the signs of all z_i $(i = 1, \ldots, 5)$ in (21) are changed into a negative. Thus, we can notice that the coupling stiffness elements $\boldsymbol{K}_{\mathrm{o}y\alpha}$, $\boldsymbol{K}_{\mathrm{o}z\beta}$ and $\boldsymbol{K}_{\mathrm{o}\gamma\alpha}$ cannot be arbitrarily planned, and also their signs changes from positive to negative or *vice versa* in comparison to the previous case.

3.2.2. T-type peg. When the hand grasps the left-side of the peg and the compliance center lies in the point $\boldsymbol{O}_3$ of Fig. 6, we can identically analyze the stiffness relation between the operational space and the fingertip space similar to the case of Fig. 5a. Also, if the hand grasps the right-side of the peg for the same compliance center $\boldsymbol{O}_3$, we can identically analyze the stiffness relation between the operational space and the fingertip space as in the case of Fig. 5b.

On the other hand, when the hand grasps the left-side of the peg and the compliance center is moved to the point $\boldsymbol{O}_4$, the sign of the kinematic influence coefficients z_1 and z_4 in (21) changes from positive to negative or *vice versa*. Also, if the hand grasps the right-side of the peg for the same compliance center $\boldsymbol{O}_4$,

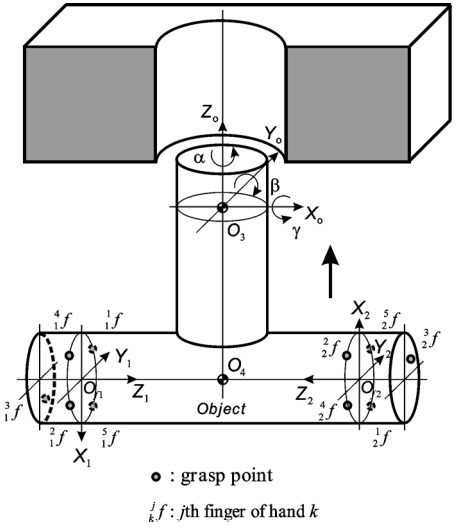

Figure 6. A perpendicular peg-in-hole task using two multi-fingered hands in 3D space.

the sign of the kinematic influence coefficients z_1, z_3, and z_4 in (21) changes from positive to negative or *vice versa*. Thus, we can notice that the coupling stiffness elements $\boldsymbol{K}_{o y\alpha}$, $\boldsymbol{K}_{o z\beta}$ and $\boldsymbol{K}_{o\gamma\alpha}$ can be arbitrarily specified, but $\boldsymbol{K}_{o x\beta}$ and $\boldsymbol{K}_{o y\gamma}$ still cannot be arbitrarily planned in those cases. Specifically, $\boldsymbol{K}_{o x\beta}$ is always positive and $\boldsymbol{K}_{o y\gamma}$ is always negative.

As a result, in assembly tasks using multi-fingered hands, we can conclude that the compliance characteristics in the operational space are different according to the grasp geometry and, also, it is closely associated with the compliance center.

4. COMPLIANCE PLANNING FOR HAND-WRITING TASKS

4.1. Hand-writing task

When a character is written by a pen grasped by multi-fingered hands, the pen should be stably picked up and, simultaneously, it should be properly handled to write characters. Sometimes, we should use the combination of the arm and hand to draw some large characters or pictures. Usually, the normal writing task is classified into three control modes. The first control mode is to approach the preparatory grasp position, which ensures that grasping is achieved as easily as possible. In this approach mode, all arm and hand joints are position controlled. The second control mode is grasping and picking up the pen. Finally, the third control mode is manipulating in the free and constrained spaces. Here, compliant motion control is necessary for dextrously manipulating the pen and effectively writing the given character.

To write a character with a pen, there are various grasp styles as shown in Fig. 7. However, the selection of a useful grasp style is very important to stably write a

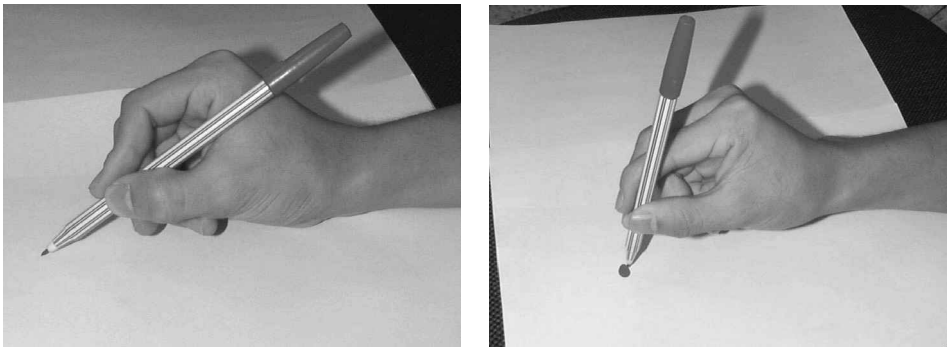

(a) (b)

Figure 7. Grasp styles of a pen by multi-fingered hands.

character. Most people prefer the grasp style of Fig. 7a when they write a character with a pen. In Fig. 7a, since the tail of the pen is constrained by the saddle between the thumb and index finger, we can intuitively see that the motion of the grasped pen can be easily balanced during the writing process. From this viewpoint, the saddle supporting the pen can be modeled as a virtual finger with 1 passive d.o.f. On the other hand, the grasp configuration shown in Fig. 7b has no constrained surface. Usually, the grasp style of Fig. 7a is better to write a precision character than the grasp style of Fig. 7b.

In this paper, we consider the writing task using fingers as shown in Fig. 7a in a quasi-static state. Also, we assume that the contact style of each fingertip is a point contact with friction and the positions of the grasped points do not change during the writing process.

4.2. Compliance planning for effective writing

Consider the grasp configuration presented in Fig. 8. Figure 9 shows the grasp posture shown in the section A–A'. Specifically, we can find that the tips of the thumb and index fingers are usually lying on the surface of the second and first quarter of the pen, respectively, and also the middle finger contacts the fourth quarter. In Fig. 8, note that the motion constraint provided by the saddle is very important to guarantee the stability of a pen during the writing process.

First, define the motion constraint as a virtual finger with passive compliance characteristics (Fig. 10). We model the contact point between the pen and the virtual finger as a high-pair joint that slides in the z-direction and rotates in the x- and y-directions. Then, the given writing tasks can be modeled as a manipulating problem by four-fingered hands. Based on the independent finger-based compliance control scheme [11], we analyze the stiffness characteristics for the defined writing task in Fig. 8. Particularly, the specified stiffness characteristics can be effectively implemented by the independent joint-based compliance control scheme presented in Ref. [23].

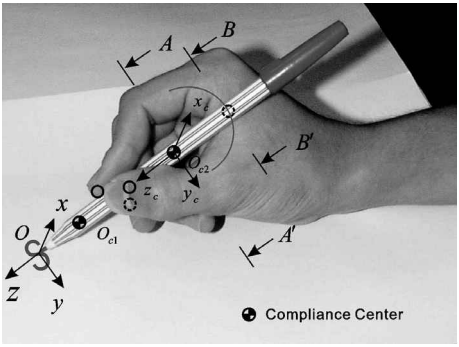

Figure 8. Writing task with a pen using multi-fingered hand.

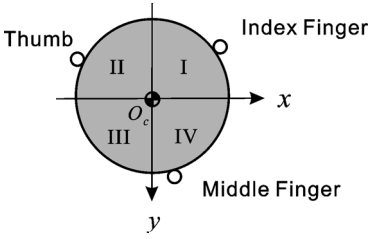

Figure 9. Grasp posture viewed in the section A–A'.

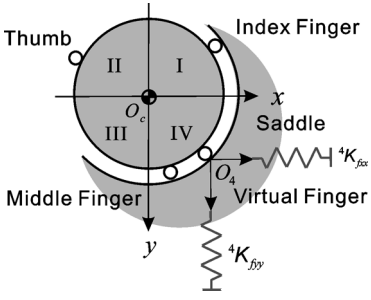

Figure 10. Virtual finger model viewed in the section B–B'.

Generally, to write a character, translational and rotational motions of the grasped pen are necessary. Also, we can observe some features of the writing task as follows. Assume that the xy-coordinates in Fig. 9 denote the horizontal plane. The translational motions in the x- and y-directions of the grasped pen are constrained by the saddle between the thumb and index finger, and thus the x-directional motion of the grasped pen is modulated by a combination of the translational motion in the z-direction and the rotational motion in the y-direction. Also, it is natural that the y-directional motion of the grasped pen is modulated by a combination of the translational motion in the z-direction and the rotational motion in the x-direction. The rotational motion for the z-direction is usually unused during the writing process. From this viewpoint, the motions of the other directions can be induced by

the combination of the three motions (i.e. z-translational, and x- and y-rotational motions).

Based on the above analysis, we analyze the stiffness map for the given writing task. When the compliance center lies in the $\boldsymbol{O}_{c1}$ position that is located in the range between the tip of the pen and the grasped points, a 6×6 stiffness matrix in the operational space of the pen can be planned as follows:

$$\begin{bmatrix} \boldsymbol{K}_{oxx} & \boldsymbol{K}_{oxy} & \boldsymbol{K}_{oxz} & \boldsymbol{K}_{ox\gamma} & \boldsymbol{K}_{ox\beta} & \boldsymbol{K}_{ox\alpha} \\ \boldsymbol{K}_{oyx} & \boldsymbol{K}_{oyy} & \boldsymbol{K}_{oyz} & \boldsymbol{K}_{oy\gamma} & \boldsymbol{K}_{oy\beta} & \boldsymbol{K}_{oy\alpha} \\ \boldsymbol{K}_{ozx} & \boldsymbol{K}_{ozy} & \boldsymbol{K}_{ozz} & \boldsymbol{K}_{oz\gamma} & \boldsymbol{K}_{oz\beta} & \boldsymbol{K}_{oz\alpha} \\ \boldsymbol{K}_{o\gamma x} & \boldsymbol{K}_{o\gamma y} & \boldsymbol{K}_{o\gamma z} & \boldsymbol{K}_{o\gamma\gamma} & \boldsymbol{K}_{o\gamma\beta} & \boldsymbol{K}_{o\gamma\alpha} \\ \boldsymbol{K}_{o\beta x} & \boldsymbol{K}_{o\beta y} & \boldsymbol{K}_{o\beta z} & \boldsymbol{K}_{o\beta\gamma} & \boldsymbol{K}_{o\beta\beta} & \boldsymbol{K}_{o\beta\alpha} \\ \boldsymbol{K}_{o\alpha x} & \boldsymbol{K}_{o\alpha y} & \boldsymbol{K}_{o\alpha z} & \boldsymbol{K}_{o\alpha\gamma} & \boldsymbol{K}_{o\alpha\beta} & \boldsymbol{K}_{o\alpha\alpha} \end{bmatrix}$$

$$= \begin{bmatrix} \otimes & 0 & 0 & 0 & -\psi_1 & \otimes \\ 0 & \otimes & 0 & +\psi_2 & 0 & \otimes \\ 0 & 0 & S & 0, \pm\psi_3 & 0, \pm\psi_4 & 0 \\ 0 & +\psi_2 & 0, \pm\psi_3 & L & 0, \pm\psi_5 & \otimes \\ -\psi_1 & 0 & 0, \pm\psi_4 & 0, \pm\psi_5 & L & \otimes \\ \otimes & \otimes & 0 & \otimes & \otimes & \otimes \end{bmatrix}, \tag{23}$$

where ψ_i $(i = 1, 2, \ldots, 5)$ are all positive, and S and L are determined by considering the task characteristic for each direction [12–14]. The symbol $\otimes$ in (23) implies unimportant stiffness elements in the writing task by structurally determined motion constraints. $\boldsymbol{K}_{o\gamma\gamma}$ and $\boldsymbol{K}_{o\beta\beta}$ denote the rotational stiffness elements in the x- and y-direction, respectively.

In (23), we can notice that the important stiffness elements for the writing task are $\boldsymbol{K}_{ozz}$, $\boldsymbol{K}_{o\gamma\gamma}$, $\boldsymbol{K}_{o\beta\beta}$ and the coupling stiffness elements relating those elements. By constructing (21) for this grasp configuration, the coupling stiffness elements $\boldsymbol{K}_{ox\beta}$ and $\boldsymbol{K}_{oy\gamma}$ can be specified as:

$$\boldsymbol{K}_{ox\beta} = -z_1{}^1\boldsymbol{K}_{fxx} - z_2{}^2\boldsymbol{K}_{fxx} - z_3{}^3\boldsymbol{K}_{fxx} - z_4{}^4\boldsymbol{K}_{fxx}, \tag{24}$$

and:

$$\boldsymbol{K}_{oy\gamma} = +z_1{}^1\boldsymbol{K}_{fyy} + z_2{}^2\,\boldsymbol{K}_{fyy} + z_3{}^3\boldsymbol{K}_{fyy} + z_4{}^4\boldsymbol{K}_{fyy}, \tag{25}$$

from the analysis given by (10) and (23), where z_i denotes the elements of position vectors directing from the ith finger contact position to the task position, and they are given all positive. Therefore, when the compliance center is located at $\boldsymbol{O}_{c1}$, $\boldsymbol{K}_{ox\beta}$ and $\boldsymbol{K}_{oy\gamma}$ should always be specified as negative and positive values, respectively.

However, if the compliance center moves to the $\boldsymbol{O}_{c2}$ region, which denotes the inner range of the grasp configuration formed by the grasp points, $\boldsymbol{K}_{ox\beta}$ and $\boldsymbol{K}_{oy\gamma}$ can be changed as:

$$\boldsymbol{K}_{ox\beta} = z_1{}^1\boldsymbol{K}_{fxx} + z_2{}^2\boldsymbol{K}_{fxx} + z_3{}^3\boldsymbol{K}_{fxx} - z_4{}^4\boldsymbol{K}_{fxx}, \tag{26}$$

and:

$$\boldsymbol{K}_{\mathrm{o}y\gamma} = -z_1{}^1\boldsymbol{K}_{\mathrm{f}yy} - z_2{}^2\boldsymbol{K}_{\mathrm{f}yy} - z_3{}^3\boldsymbol{K}_{\mathrm{f}yy} + z_4{}^4\boldsymbol{K}_{\mathrm{f}yy}. \tag{27}$$

Thus, those coupling elements can be designed as arbitrary values since the positions of z have different signs. As a result, the stiffness matrix in the operational space of the pen can be planned as:

$$\begin{bmatrix} \boldsymbol{K}_{\mathrm{o}xx} & \boldsymbol{K}_{\mathrm{o}xy} & \boldsymbol{K}_{\mathrm{o}xz} & \boldsymbol{K}_{\mathrm{o}x\gamma} & \boldsymbol{K}_{\mathrm{o}x\beta} & \boldsymbol{K}_{\mathrm{o}x\alpha} \\ \boldsymbol{K}_{\mathrm{o}yx} & \boldsymbol{K}_{\mathrm{o}yy} & \boldsymbol{K}_{\mathrm{o}yz} & \boldsymbol{K}_{\mathrm{o}y\gamma} & \boldsymbol{K}_{\mathrm{o}y\beta} & \boldsymbol{K}_{\mathrm{o}y\alpha} \\ \boldsymbol{K}_{\mathrm{o}zx} & \boldsymbol{K}_{\mathrm{o}zy} & \boldsymbol{K}_{\mathrm{o}zz} & \boldsymbol{K}_{\mathrm{o}z\gamma} & \boldsymbol{K}_{\mathrm{o}z\beta} & \boldsymbol{K}_{\mathrm{o}z\alpha} \\ \boldsymbol{K}_{\mathrm{o}\gamma x} & \boldsymbol{K}_{\mathrm{o}\gamma y} & \boldsymbol{K}_{\mathrm{o}\gamma z} & \boldsymbol{K}_{\mathrm{o}\gamma\gamma} & \boldsymbol{K}_{\mathrm{o}\gamma\beta} & \boldsymbol{K}_{\mathrm{o}\gamma\alpha} \\ \boldsymbol{K}_{\mathrm{o}\beta x} & \boldsymbol{K}_{\mathrm{o}\beta y} & \boldsymbol{K}_{\mathrm{o}\beta z} & \boldsymbol{K}_{\mathrm{o}\beta\gamma} & \boldsymbol{K}_{\mathrm{o}\beta\beta} & \boldsymbol{K}_{\mathrm{o}\beta\alpha} \\ \boldsymbol{K}_{\mathrm{o}\alpha x} & \boldsymbol{K}_{\mathrm{o}\alpha y} & \boldsymbol{K}_{\mathrm{o}\alpha z} & \boldsymbol{K}_{\mathrm{o}\alpha\gamma} & \boldsymbol{K}_{\mathrm{o}\alpha\beta} & \boldsymbol{K}_{\mathrm{o}\alpha\alpha} \end{bmatrix}$$

$$= \begin{bmatrix} \otimes & 0 & 0 & 0 & 0, \pm\psi_1 & \otimes \\ 0 & \otimes & 0 & 0, \pm\psi_2 & 0 & \otimes \\ 0 & 0 & S & 0, \pm\psi_3 & 0, \pm\psi_4 & 0 \\ 0 & 0, \pm\psi_2 & 0, \pm\psi_3 & L & 0, \pm\psi_5 & \otimes \\ 0, \pm\psi_1 & 0 & 0, \pm\psi_4 & 0, \pm\psi_5 & L & \otimes \\ \otimes & \otimes & 0 & \otimes & \otimes & \otimes \end{bmatrix}. \tag{28}$$

From (28), we can notice that the coupling stiffness elements, $\boldsymbol{K}_{\mathrm{o}x\beta}$ and $\boldsymbol{K}_{\mathrm{o}y\gamma}$, can be specified as zero and, thus, the unwanted translational motion caused by the rotational motions in the x- and y-directions can be removed. Also, we can observe that this effect can be obtained by defining the supporting saddle as a virtual finger. Since this effect can improve the stability of a pen in the writing process, it can be considered as an analytical condition for the rotational stability in multi-fingered manipulations [27].

As a result, we can say that the grasp configuration with the compliance center $\boldsymbol{O}_{\mathrm{c}2}$ is useful for writing characters. It can be observed from (28) that at least eight independent stiffness elements need to be controlled. They correspond to $\boldsymbol{K}_{\mathrm{o}zz}$, $\boldsymbol{K}_{\mathrm{o}\gamma\gamma}$, $\boldsymbol{K}_{\mathrm{o}\beta\beta}$, $\boldsymbol{K}_{\mathrm{o}x\beta}$, $\boldsymbol{K}_{\mathrm{o}y\gamma}$, $\boldsymbol{K}_{\mathrm{o}z\gamma}$, $\boldsymbol{K}_{\mathrm{o}z\beta}$ and $\boldsymbol{K}_{\mathrm{o}\gamma\beta}$.

Now, it is necessary to measure how many fingers are required to achieve the given stiffness characteristic of the writing task. A fundamental necessary condition for manipulating on object by multi-fingered hands was presented [11].

Through the above analysis, we can conclude that the writing task can be more effectively achieved by four-fingered hands considering the grasp configuration of Fig. 7a since there are more stiffness elements in the four fingers than required to modulate the eight operational stiffness elements.

5. CONCLUDING REMARKS

A task-based guideline of specifying compliance characteristics in the operational space of multi-fingered hands was presented in this paper. Through analyzing the

stiffness relation between the operational space and the fingertip space of multi-fingered hands, it is shown that some stiffness elements in the operational space are appropriately planned, but some of the coupling stiffness elements cannot be planned arbitrarily. As a result, we can conclude that the operational stiffness matrix should be carefully specified by considering the grasp geometry of multi-fingered hands, and that the location of the RCC point is crucial for successful grasping and manipulation tasks. A couple of examples are illustrated to corroborate the effectiveness of the proposed task-based compliance planning algorithms.

Acknowledgements

This work was supported by the Korea Health 21 R&D Project, Ministry of Health and Welfare, Republic of Korea, under Grant 02-PJ3-PG6-EV04-0003.

REFERENCES

1. T. Yoshikawa and X.-Z. Zheng, Coordinated dynamic hybrid position/force control for multiple robot manipulators handling one constrained object, *Int. J. Robotics Res.* **12** (3), 219–230 (1993).
2. H. Maekawa, K. Tanie and K. Komoria, Dynamic grasping force control using tactile feedback for grasp of multifingered hand, in: *Proc. IEEE Int. Conf. on Robotics and Automation*, Minneapolis, MN, pp. 2462–2469 (1996).
3. S. L. Jiang, K. K. Choi and Z. X. Li, Coordinated motion generation for multifingered manipulation using tactile feedback, in: *Proc. IEEE Int. Conf. on Robotics and Automation*, Detroit, MI, pp. 3032–3037 (1999).
4. J. L. Pons, R. Ceres and F. Pfeiffer, Multifingered dexterous robotics hand design and control: a review, *Robotica* **17**, 661–674 (1999).
5. M. R. Cutkosky and I. Kao, Computing and controlling the compliance of a robotic hand, *IEEE Trans. Robotics Automat.* **5** (2), 151–165 (1989).
6. M. Kaneko, N. Imamura, K. Yokoi and K. Tanie, A realization of stable grasp based on virtual stiffness model by robot fingers, in: *Proc. IEEE Int. Workshop on Advanced Motion Control*, pp. 156–163 (1990).
7. I. Kao, M. R. Cutkosky and R. S. Johansson, Robotic stiffness control and calibration as applied to humnan grasping tasks, *IEEE Trans. Robotics Automat.* **13** (4), 557–566 (1997).
8. D. E. Whitney, Quasi-static assembly of compliantly supported rigid parts, *J. Dyn. Syst. Meas. Control* **104**, 65–77 (1982).
9. H. Asada and Y. Kakumoto, The dynamic analysis and design of a high-speed insertion hand using the generalized centroid and virtual mass, *J. Dyn. Syst. Meas. Control* **112**, 646–652 (1990).
10. T. Matsuoka, T. Hasegawa, T. Kiriki and K. Honda, Mechanical assembly based on motion primitives of multi-fingered hand, in: *Proc. Advanced Intelligent Mechatronics*, Villa Olmo (1997).
11. B.-H. Kim, B.-J. Yi, S.-R. Oh and I. H. Suh, Independent finger and independent joint-based compliance control of multi-fingered robot hands, *IEEE Trans. Robotics Automat.* **19** (2), 185–199 (2003).
12. J. D. Schutter and H. V. Brussel, Compliant robot motion I. A formalism for specifying compliant motion tasks, *Int. J. Robotics Res.* **7** (4), 3–17 (1988).
13. J. D. Schutter and H. V. Brussel, Compliant robot motion II. A control approach based on external control loops, *Int. J. Robotics Res.* **7** (4), 18–33 (1988).

14. K. B. Shimoga and A. A. Goldenberg, Grasp admittance center: choosing admittance center parameters, in: *Proc. Am. Control Conf.*, Boston, MA, pp. 2527–2532 (1991).
15. M. H. Ang, Jr. and G. B. Andeen, Specifying and achieving passive compliance based on manipulator structure, *IEEE Trans. Robotics Automat.* **11** (4), 504–515 (1995).
16. B.-H. Kim, B.-J. Yi, S.-R. Oh and I. H. Suh, Fundamentals and analysis of compliance characteristics for multi-fingered hands, in: *Proc. IEEE Int. Conf. on Robotics and Automation*, Seoul, pp. 3034–3041 (2001).
17. S. Huang and J. M. Schimmels, The bounds and realization of spatial stiffnesses achieved with simple springs connected in parallel, *IEEE Trans. Robotics Automat.* **14** (3), 466–475 (1998).
18. J. M. Selig, The spatial stiffness matrix from simple stretched springs, in: *Proc. IEEE Int. Conf. on Robotics and Automation*, San Francisco, CA, pp. 3314–3319 (2000).
19. R. G. Roberts, On the normal form of a spatial stiffness matrix, in: *Proc. IEEE Int. Conf. on Robotics and Automation*, Washington, DC, pp. 556–561 (2002).
20. R. A. Freeman and D. Tesar, Dynamic modeling of serial and parallel mechanisms/robotics systems, Part I — methodology, Part II — applications, in: *Proc. 20th ASME Biennial Mechanisms Conf., Trends and Development in Mechanisms, Machines, and Robotics*, DE-Vol. 15-2, Orlando, FL, pp. 7–21 (1988).
21. B.-J. Yi, I. D. Walker, D. Tesar and R. A. Freeman, Geometric stability in force control, in: *Proc. IEEE Int. Conf. on Robotics and Automation*, Sacramento, CA, pp. 281–286 (1991).
22. J. K. Salisbury, Active stiffness control of manipulator in Cartesian coordinates, in: *Proc. IEEE 19th Conf. on Decision and Control*, Detroit, MI, pp. 95–100 (1980).
23. B.-R. So, B.-J. Yi, S.-R. Oh and I. H. Suh, An independent joint-based compliance control method for a five-bar finger mechanism via redundant actuators, in: *Proc. IEEE Int. Conf. on Robotics and Automation*, pp. 2140–2146 (1999).
24. S.-F. Chen and I. Kao, Geometrical method for modeling of asymmetric 6×6 Cartesian stiffness matrix, in: *Proc. IEEE/RSJ Int. Conf. on Intelligent Robots and Systems*, Takamatsu, pp. 1217–1222 (2000).
25. B.-H. Kim, B.-J. Yi, S.-R. Oh and I. H. Suh, Task-based compliance planning for multi-fingered hands, in: *Proc. IEEE Int. Conf. on Robotics and Automation*, Seoul, pp. 2614–2621 (2001).
26. B.-H. Kim, S.-R. Oh, B.-J. Yi and I. H. Suh, Compliance planning for dextrous assembly tasks using multi-fingered robot hands, *Int. J. Intelligent Automat. Soft Comput.* **8** (1), 51–64 (2002).
27. M. M. Svinin, K. Ueda and M. Kaneko, Analytical conditions for the rotational stability of an object in multi-finger grasping, in: *Proc. IEEE Int. Conf. on Robotics and Automation*, Detroit, MI, pp. 257–262 (1999).

ABOUT THE AUTHORS

Byoung-Ho Kim received the BS and MS degrees from the Department of Electronics Engineering of Kumoh National University of Technology, Kumi, Korea, in 1985 and 1994, respectively. In 2001, he received PhD degree from the Department of Electronics Engineering of Hanyang University, Seoul, Korea. From 1989 to 1993, he was a researcher with the Department of Research and Development of LG Innotek, Kumi, Korea. From 1995 to 1999, he joined a humanoid development project with the Intelligent System Control Research Center of Korea Institute of Science and Technology, Seoul, Korea. He is currently a Japan Society for the Promotion of Science Post-Doctoral Fellow with the Department of Robotics of Ritsumeikan University, Kusatsu, Shiga, Japan. His research interests include multi-fingered hands, biomimetic robotic systems, soft manipulation, mobile manipulation, intelligent control for humanoids, and medical science. He is a member of the IEEE, the Electronics Engineers of Korea, and the Institute of Control, Automation and Systems Engineers of Korea.

Byung-Ju Yi received the BS degree from the Department of Mechanical Engineering, Hanyang University, Seoul, Korea in 1984, and the MS and PhD degrees from the Department of Mechanical Engineering, University of Texas at Austin, in 1986 and 1991, respectively. From January 1991 to August 1992, he was a Post-Doctoral Fellow with the Robotics Group, University of Texas at Austin. From September 1992 to February 1995, he was an Assistant Professor in the Department of Mechanical and Control Engineering, Korea Institute of Technology and Education, Chonan, Chungnam, Korea. In March 1995, he joined the Department of Control and Instrumentation Engineering, Hanyang University. Currently, he is an Associate Professor with the School of Electrical Engineering and Computer Science, Hanyang University. His research interests include multiple arms, parallel manipulators, multi-fingered hands, micromanipulators, mobile manipulation, biomimetic robotic systems and sport science.

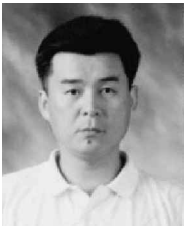

Sang-Rok Oh received the BS degree in Electronic Engineering from Seoul National University, Seoul, Korea, in 1980, and the MS and PhD degrees in Electrical and Electronic Engineering from the Korea Advanced Institute of Science and Technology (KAIST), Daeduk, Korea, in 1982 and 1987, respectively. He worked as a Research Associate at the Systems Control Laboratory, KAIST, for 10 months in 1987, conducting the design and implementation of multiprocessor-based automatic assembly machine for micro electronic components and a robotic control system for multilegged locomotion. In 1988, he joined the Korea Institute of Science and Technology (KIST) and has been working as a Principal Research Engineer at the Intelligent System Control Research Center (ISCRC), KIST. Since 2000, he has been a Head of ISCRC, KIST. In 1999, he also became a Director of the Bio-mimetic Control National Research Laboratory, which was designated by the Ministry of Science and Technology, Korea. He was a Visiting Scientist at the T. J. Watson Research Center, IBM, Yorktown Heights, NY, from 1991 to 1992, conducting precision assembly using the magnetically levitated robot twist. He also worked as a Visiting Scientist at the Mechanical Engineering Laboratory, Tsukuba, Japan, for 3 months in 1995, investigating the area of mobile manipulation systems. His research interests include biomimetic control of intelligent robots, mobile manipulation, multifingered robotic hands and service robots. He is a member of the IEEE, the Korea Institute of Electrical Engineering, the Korea Fuzzy Logic and Intelligent System Society, and the Institute of Control, Automation and System Engineering, Korea.

Il Hong Suh was born in Seoul, Korea. He received the BS degree in Electronics Engineering from Seoul National University, Seoul, Korea, in 1977, and the MS and PhD degrees in electrical engineering from the Korea Institute of Science and Technology (KAIST), Seoul, in 1979 and 1982, respectively. From 1982 to 1985, he was a Senior Research Engineer at the Technical Center of Daewoo Heavy Industries, Ltd, Inchon, Korea, where he was involved in research on machine vision and the development of the Daewoo NOVA10 robot controller. From 1985 to 1986, he was with the Systems Control Laboratory, KAIST, as a part-time Research Fellow for an automation-related Korea National Project. In 1987, he was a Visiting Research Fellow at the Robotics Division, CRIM, University of Michigan, Ann Arbor. From 1998 to 2000, he served as Vice Dean of Academic Affairs, Ansan campus, Hanyang University. Since 2000, he has served as a Director of the Center for Hanyang Business Incubation. He as also been with the School of Electrical and Computer Engineering, Hanyang University, Korea, where he is a Professor. His research interests include sensor-based control of robot manipulators, artificial life, haptics, intelligent control involving fuzzy logics, neural networks and reinforcement learning.